ALEXANDRITE-RING-LASER-BASED FE DOPPLER LIDAR FOR MOBILE/AIRBORNE DEPLOYMENT

Xinzhao Chu

University of Colorado, CIRES, 216 UCB, Boulder, CO 80309, USA, Email: Xinzhao.Chu@Colorado.edu

ABSTRACT

Global temperature and wind profiling through the middle and upper atmosphere with high accuracy, precision, and resolution is crucial in the validation and improvement of global atmosphere models for climate study. Resonance fluorescence Doppler lidars, like the dye-laser-based Na wind/temperature lidar, have proven the unmatched capabilities in high-resolution measurements of wind and temperature in the mesopause region at a few locations. To achieve such measurements globally and extend to stratosphere, an Fe Doppler lidar based on solid-state alexandrite ring-laser has compelling reasons to be an attractive resonance fluorescence Doppler lidar. In this paper, we discuss the principle, feasibility, and potentials of a proposed Fe Doppler lidar for airborne and groundbased mobile deployment. The combination of state-of-the-art narrowband laser transmitter with holographic scanning receiver and high Fe abundance and short operating wavelength make the Fe Doppler lidar an ideal candidate for the next-generation lidar.

1. INTRODUCTION

Human induced changes in the global climate are among the most significant scientific challenges of this century. Models of the global atmosphere are used to understand these issues and to project the future state of the climate. Global measurements of temperature and wind are needed to provide crucial tests of models and the means to monitor climate change throughout the atmosphere. Similarly, dynamic parameters like gravity waves, tides, and aerosols inferred from these measurements provide important input to the models. The acquisition of global temperature and wind data in the middle and upper atmosphere demands high-accuracy, high-precision and high-resolution Doppler lidar with great mobility. This is beyond the capability of any existing lidar system.

The National Science Foundation new aircraft, HIAPER (High-Performance Instrumented Airborne Platform for Environmental Research), provides a great opportunity for making such lidar observations globally. HIAPER is a Gulfstream-V business jet with exceptionally long flight range (~11,000 km) and a high cruising altitude up to 15 km. It can fly non-stop roundtrip missions to the North Pole or the Equator from the northern hemisphere, and roundtrip mission to the South Pole when based in the southern hemisphere. Therefore, developing a Doppler lidar for HIAPER is clearly very attractive.

Resonance fluorescence lidars including narrowband Doppler lidars and broadband Boltzmann lidars have made significant contributions to the middle and upper atmosphere study [1]. In the choice of future Doppler lidars among Na, Fe, and K in the mesopause region, the combination of high abundance, short operating wavelength (thus strong molecular scattering with large Rayleigh temperature range), high laser power, high wind and temperature sensitivity, and deep Fraunhofer line in solar spectrum, makes the Fe Doppler lidar an ideal candidate [2]. This choice is further endorsed by the readiness of solid-state alexandrite ring laser technology and holographic scanner technology. We propose to develop an alexandrite-ring-laser-based Fe Doppler lidar operating at 372 nm to profile temperature, wind, meteoric Fe density, aerosols and clouds throughout the stratosphere, mesosphere, and lower thermosphere. It is designed for deployment on the HIAPER aircraft as well as for groundbased mobile deployment. In fact, an Fe temperature lidar operating at a weaker Fe 386 nm line, developed by the IAP scientists, have shown promising performance [3].

2. PRINCIPLE OF FE DOPPLER LIDAR

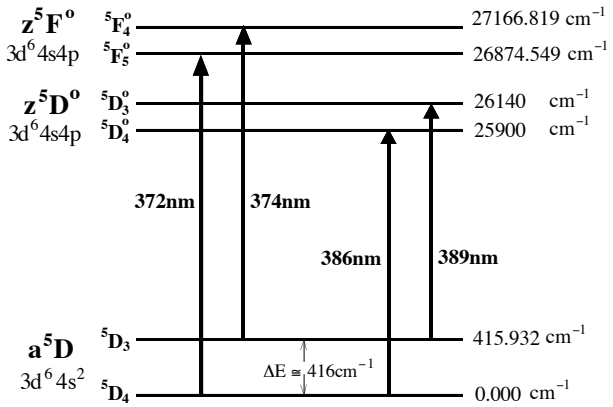

Figure 1. Energy level diagram for atomic ^{56}Fe isotope.

The proposed Fe Doppler lidar is based on the strong 372 nm absorption line originating from the lowest sublevel of Fe ground state a^5D_4 to an excite state z^5F_5 (see Fig. 1). The effective cross-section of the 372 nm line is nearly 2.5 times of the 386 nm line (from a^5D_4 to z^5D_4), thus, providing much stronger lidar return signals. Fe atoms have four naturally stable isotopes ^{56}Fe, ^{54}Fe, ^{57}Fe, and ^{58}Fe with natural abundance of 91.75%, 5.85%, 2.12%, and 0.28%, respectively. There are isotope line shifts between these isotopes. For the simplicity of explanation, we use the ^{56}Fe isotope to

show the energy levels and absorption cross-section. The influence of isotope shifts will be discussed later. The nuclear spin of ^{56}Fe is zero, thus, ^{56}Fe has no hyperfine splitting, resulting in relatively simple energy diagram as shown in Fig. 1.

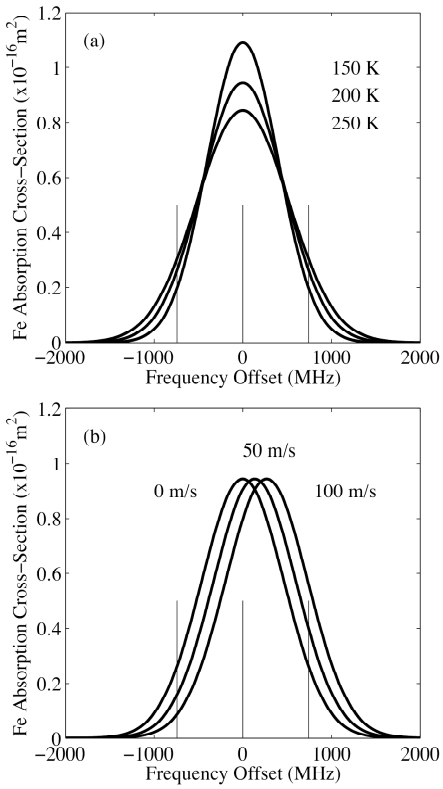

Figure 2. (a) ^{56}Fe absorption cross-section for three temperature at V_R = 0/ms. (b) ^{56}Fe absorption cross-section for three radial wind at T = 200 K.

The Fe Doppler lidar is based on the well-known Doppler effect: the Fe absorption cross-section σ_{abs} is Doppler broadened by the Maxwellian thermal velocity distribution and the central frequency is Doppler shifted by the macro radial wind velocity V_R.

$$\sigma_{abs}(f_L) = \frac{1}{\sqrt{2\pi}\sigma_D}\frac{e^2 f_{ik}}{4\varepsilon_0 m_e c}\exp\left(-\frac{\left[f_{Fe} - f_L(1-V_R/c)\right]^2}{2\sigma_D^2}\right) \quad (1)$$

where $\sigma_D = \sqrt{k_B T / M_{Fe}\lambda_0^2}$ is the rms width of the Doppler broadening, k_B is the Boltzmann constant, T is the temperature, M_{Fe} is the Fe mass, λ_0=372.0993 nm is the wavelength in vacuum of the ^{56}Fe 372 nm line, V_R is the radial velocity along the line of sight, f_{Fe} is the central frequency of the Fe resonance line, f_L is the laser frequency, c is the light speed, e is the electron charge, m_e is the electron mass, ε_0 is the permittivity of free space, and f_{ik} is the oscillator strength for the Fe 372 nm line. Fig. 2 shows how the Fe absorption cross-section varies with different temperatures and winds. The center frequency is the resonance frequency of the ^{56}Fe 372 nm line. By probing the Doppler width and the Doppler shift of the Fe absorption line at 372 nm, atmosphere temperature and wind can be inferred. This can be done by either scanning the laser frequency through the absorption line [3] or probing the spectrum at three frequencies, i.e., the 3-frequency technique used in the Na wind/temperature lidar [4] and the K Doppler lidar [5]. The three frequencies (f_S, $f_S\pm\Delta f$) chosen for the Fe Doppler lidar are shown as the thin vertical lines in Fig. 2, based on the analysis of [2]. Here, f_S is the central frequency and Δf is the frequency offset of the two wing frequencies relative to the central frequency. It can be chosen to minimize the measurement errors depending on experimental conditions [2]. The temperature (R_T) and wind (R_W) metrics are defined as

$$R_T = \frac{N_S(f_S+\Delta f)N_S(f_S-\Delta f)}{{N_S}^2(f_S)} \quad (2)$$

$$R_W = \frac{\ln\left[N_S(f_S-\Delta f)/N_S(f_S+\Delta f)\right]}{\ln\left[N_S(f_S-\Delta f)N_S(f_S+\Delta f)/{N_S}^2(f_S)\right]} \quad (3)$$

where N_S is the signal photon count at different frequencies. These two ratios are sensitive functions of temperature and wind, respectively (Fig. 3).

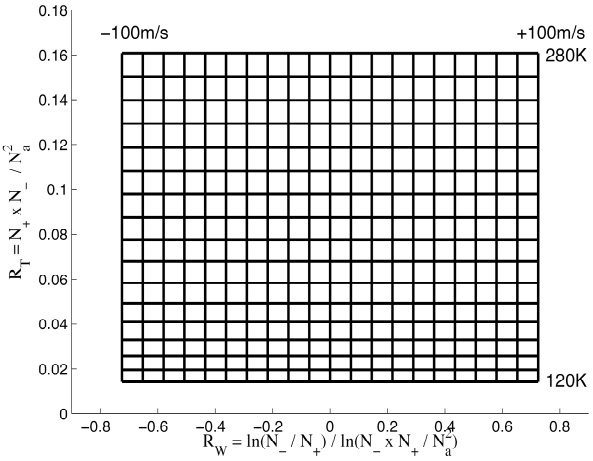

Figure 3. Ratios R_T and R_W for temperature range of 120-280 K and radial velocity range of -100 to 100 m/s.

For an ideal case of pure Gaussian lineshape, R_T is independent of radial wind and R_W is independent of temperature. Thus, R_T is insensitive to the laser frequency tuning error, and R_W is insensitive to the laser linewidth error. In reality, due to the Fe isotope shifts, the 372 nm line is not perfect Gaussian, so the calibration curve shown in Fig. 3 will experience some distortion. Nevertheless, the metrics shown in Eqs. 2-3 exhibit high temperature and wind sensitivities, which make the Fe Doppler lidar an ideal choice for the Doppler lidar.

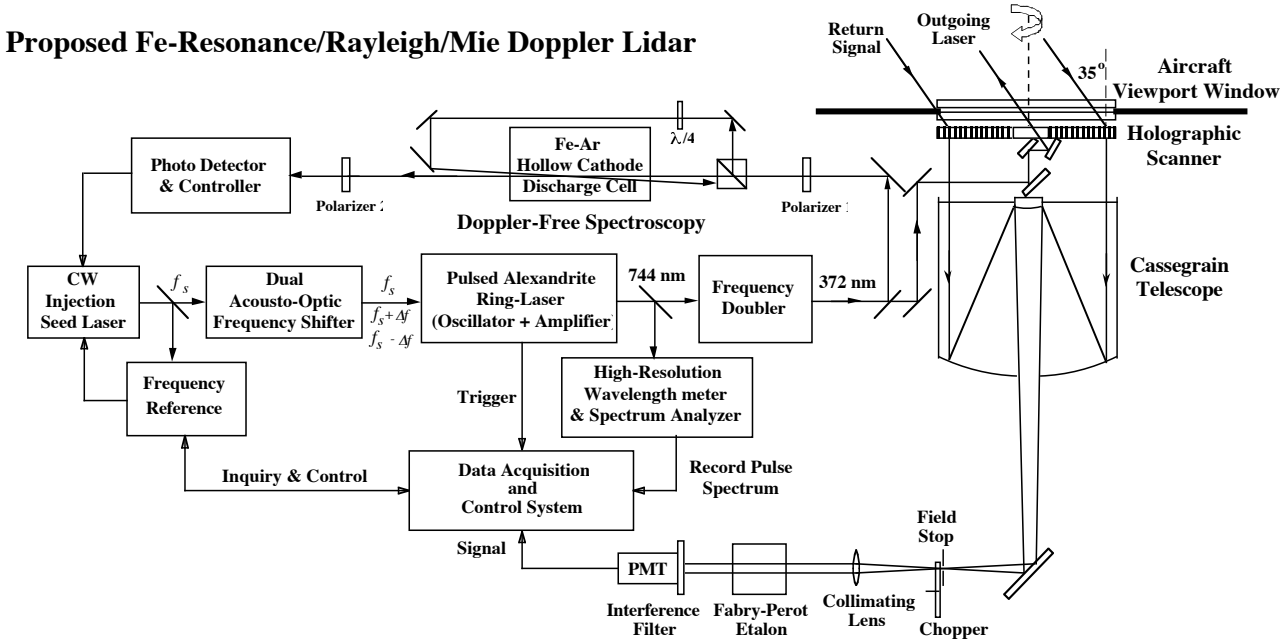

Figure 4. Proposed Fe Doppler lidar diagram with Fe Doppler-free spectroscopy at 372 nm

3. DESIGN OF FE DOPPLER LIDAR

The proposed Fe Doppler lidar is illustrated in Fig. 4. It extends the state of the art by combining an injection-seeded, frequency-doubled, alexandrite ring-laser with a holographic scanner. The seed laser is provided by an external cavity diode laser operating at the fundamental wavelength of 744 nm, whose frequency can be shifted up and down by a dual acousto-optical modulator to generate two required wing frequencies. The alexandrite laser frequency will then follow the seed laser frequency and be tuned between the peak frequency and two wing frequencies to probe the Fe line. Iodine absorption lines are available in this infrared range, and we have identified an iodine line at 13437.2949 cm^{-1} to be 611.6 MHz higher than the desired frequency of 13437.2745 cm^{-1} (corresponding to twice the Fe resonance wavelength). Thus, the iodine vapor cell can be used to provide an absolute frequency reference for the Fe Doppler lidar. To achieve both absolute frequency calibration and long-term/short-term frequency stability, a high-finesse, stabilized reference cavity and a high gain servo-loop will be employed to lock the seed laser frequency in order to compensate the poor signal-to-noise ratio of the iodine line. The lidar receiver consists of a volume phase holographic grating [6] on top of a conventional Cassegrain telescope. The holographic scanner directs the outgoing laser beam to an off-zenith angle and diffracts the return signals from that direction so that they can be collected by the zenith-pointing telescope. By rotating the holographic grating as well as the steering fixture about the telescope axis, the beam will sweep out a cone of light at the grating diffraction angle. Thus, horizontal wind can be conveniently measured. The daytime lidar operation is enabled by employing a double-etalon and spatial filters to strongly compress the solar background. The mobility of the lidar is achieved by making the lidar sufficiently compact to fit in the HIAPER aircraft or a container and sufficiently robust to tolerate the vibrations and thermal changes that accompany mobile deployment.

The alexandrite ring laser, the holographic grating, and the double etalon are all commercially available from several high-tech research companies, like Light Age, Inc., Wasatch Photonics, and Scientific Solution, Inc. Careful design and manufacture will make this proposed lidar suitable for the airborne and mobile deployment.

4. PREDICTED LIDAR PERFORMANCE

Laser frequency jitter, linewidth variations and receiver filter transmission variation can affect the accuracy of the derived temperature and wind. The lidar is designed so that these effects have a negligible impact on the measurements, say, temperature and wind accuracy of better than 1 K and 1 m/s. The measurement precision (uncertainty) is mainly determined by the signal-to-noise ratio, which depends on the signal and the background photon counts. In modeling the lidar performance, we adapt the methods used in [2] and take the error estimate equations given there. The signal and background photon counts are conservatively estimated using the actual signals measured by a broadband Fe Boltzmann lidar [7] at Rothera, Antarctica and then scaling according to the proposed and existing instrument parameters. Due to limited space inside HIAPER, the telescope size is about 40-50 cm. The expected performance of the proposed Fe Doppler lidar aboard HIAPER aircraft is listed in Tables 1 for 35° off-zenith pointing. The HIAPER cruise speed is 800 km/hr.

Table 1. Three-Frequency Fe/Rayleigh Doppler Lidar Performance at off-zenith angle of 35°

With Holographic Scanner Aboard HIAPER at 14 km	Temperature Error	Zonal & Meridional Wind Error	Vertical Resolution	Horizontal Resolution
Fe @ Night (80-96 km)	± 1.1 – 2.4 K	± 1.5 – 3.4 m/s	1 km	250 km
Rayleigh @ Night (30-65 km)	≤ ±1.8 K		1 km	250 km
Fe @ Day (80-96 km)	± 1.1 – 2.7 K	± 1.5 – 4.1 m/s	3 km	500-1000 km
Rayleigh @ Day (30-65 km)	≤ ±3.6 K		3 km	500-1000 km

5. FE DOPPLER-FREE SPECTROSCOPY

Table 2. Isotope shift of Fe 372 nm line

Isotopes	Line shift (MHz) [9]	Line shift (MHz) [8]
^{54}Fe	-711±9	-725±10
^{56}Fe	0	0
^{57}Fe	375±6	495±10
^{58}Fe	669±15	N/A

Two main issues associated with the Fe Doppler lidar are the Fe isotope shifts and the possible frequency chirp suffered by injection-seeded pulsed laser. By ignoring the isotope shifts, as large as 20 K temperature bias can be resulted. Published isotope shift data of Fe 372 nm line are summarized in Table 2. Apparently, more work is needed to determine the shift to better precision.

Frequency chirp refers to the discrepancy between the central frequency of the laser pulse and the cw injection seeding laser frequency, mainly caused by the time dependent gain. Therefore, we propose to monitor every outgoing pulse and record its spectrum by high-resolution wavelength meter and spectrum analyzer. In addition, it is desirable to achieve Doppler-free Fe spectroscopy to lock the pulse frequency directly onto the resonance frequency of the Fe 372 nm line. In light of the pioneer work by [8], we propose to use an Fe-Ar hollow cathode discharge cell (which allows much lower temperature ~ 600 K to achieve sufficient Fe vapor pressure) and saturation-polarization/absorption spectroscopy to achieve such Doppler-free spectroscopy at 372 nm. The setup is shown in Fig. 4 above the laser path, which will allow us not only to lock the laser frequency to as narrow as 33 MHz Doppler free feature, but also to enable accurate measurements of the Fe isotope shifts. [8] achieved great success with the CW frequency-double Ti:Sapphire laser at 372 nm. The pulsed alexandrite laser will pose a great challenge for the Doppler-free spectroscopy. Fortunately, since the alexandrite ring laser pulse is longer than 250 ns, which is about 4 times of the Fe radiative lifetime, it is possible to achieve the Doppler-free spectroscopy. This long pulse length also helps avoid saturation in the Fe layers, which is a major problem for current Na lidar.

6. CONCLUSIONS

The combination of state-of-the-art narrowband laser transmitter with holographic scanning receiver and high Fe abundance and short operating wavelength make the Fe Doppler lidar an ideal candidate for the next-generation lidar. This lidar combines in a single system key breakthroughs in lidar, laser and optical technology. It will be specifically engineered for deployment aboard HIAPER aircraft to globally profile temperature and wind with high-accuracy, precision, and resolution through the middle and upper atmosphere.

ACKNOWLEDGEMENTS

The author gratefully acknowledges the valuable discussions with Chester S. Gardner, Jonathan S. Friedman, Jeffrey P. Thayer, Josef Höffner, Walter Robinson, and Wentao Huang in the preparation of the proposal and manuscript. X. Chu is partly supported by the United States National Science Foundation Grants ATM-03-34357 and ATM-06-02334.

REFERENCES

1. Chu, X., and G. Papen, Resonance fluorescence lidar for measurements of the middle and upper atmosphere, chapter in *Laser Remote Sensing*, edited by T. Fujii and T. Fukuchi, published by CRC Press, Taylor & Francis Group, ISBN: 0-8247-4256-7, page 179-432, 2005.

2. Gardner, C. S., Performance capabilities of middle-atmosphere temperature lidars: comparison of Na, Fe, K, Ca, Ca^+, and Rayleigh systems, *Appl. Opt.*, 43, 4941-4956, 2004.

3. Lautenbach, J., and J. Höffner, Scanning iron temperature lidar for mesopause temperature observation, *Appl. Opt.*, 43, 4559-4563, 2004.

4. She, C. Y., and J. R. Yu, Simultaneous three-frequency Na lidar measurements of radial wind and temperature in the mesopause region, Geophys. Res. Lett., 21, 1771-1774, 1994.

5. Friedman, J. S. et al., Potassium Doppler-resonance lidar for the study of the mesosphere and lower thermosphere at the Arecibo Observatory, *J. Atoms. Sol.-Terr. Phys., 65*, 1411–1424, 2003.

6. Schwemmer, G. K., Holographic airborne rotating lidar instrument experiment (HARLIE), 19th ILRC paper, 1998.

7. Chu, X. et al., Fe Boltzmann temperature lidar: design, error analysis, and initial results at the North and South Poles, *Appl. Opt., 41*, 4400–4410, 2002.

8. Smeets, B., et al., Laser frequency stabilization using an Fe-Ar hollow cathode discharge cell, *Appl. Phys. B 76*, 815-819, 2003.

9. Kaletta, D., Isotopieverschiebung im eisen-I-spektrum, Diploma thesis, Univ. of Hannover, 1969.